J. Fluid Mech. (2009), *vol.* 626, *pp.* 1–20.
doi:10.1017/S0022112008004758 Printed in the United Kingdom

Exposure of internal waves on the sea surface

HWUNG-HWENG HWUNG,
RAY-YENG YANG AND IGOR V. SHUGAN†

Tainan Hydraulics Laboratory, National Cheng Kung University, 5th floor, 500, Sec. 3, Anming Road, Tainan 709, Taiwan

(Received 7 January 2008 and in revised form 21 October 2008)

We theoretically analyse the impact of subsurface currents induced by internal waves on nonlinear Stokes surface waves. We present analytical and numerical solutions of the modulation equations under conditions that are close to group velocity resonance. Our results show that smoothing of the downcurrent surface waves is accompanied by a relatively high-frequency modulation, while the profile of the opposing current is reproduced by the surface wave's envelope. We confirm the possibility of generating an internal wave forerunner that is a modulated surface wave packet. Long surface waves can create such a wave modulation forerunner ahead of the internal wave, while other relatively short surface waves comprise the trace of the internal wave itself. Modulation of surface waves by a periodic internal wavetrain may exhibit a characteristic period that is less than the internal wave period. This period can be non-uniform while the wave crosses the current zone. Our results confirm that surface wave excitation by means of internal waves, as observed at their group resonance frequencies, is efficient only in the context of opposing currents.

1. Introduction

Internal waves (IW) are one of the most interesting and inadequately studied phenomena in ocean dynamics. Though these waves exist virtually everywhere, there is rather limited experimental data that describes them. Field investigations carried out by conventional contact oceanography methods are complicated by significant technical problems. As a rule, research vessels work in rather bounded areas of the world's oceans and cannot solve the problem of reconstructing general IW pattern on a global scale.

Another line of inquiry shows great promise: the remote study of IWs by observing them at the sea surface and using contact measurements to perform relevant analyses. Many researchers have explored the ability of IWs to substantially change the wave structures that are visible on the ocean surface (see Hughes & Grant 1978; Osborne & Burch 1980; Alpers 1985). A basic example of the surface effects of IW is wide parallel bands of smooth sea surface (slicks), as well as zones that feature appreciably increased surface slopes, causing frequent wave breaking (roughness). The strongest effects may result in surface waves (SW) of metre and decimetre length.

Remote sensing instruments (radars, traditional optical devices and laser locators-lidars) can reliably detect IW surface effects at the ocean surface. At the same time, the quantification of IW parameters via remote sensing of the sea surface requires that a number of theoretical problems be solved. First, it is necessary to construct a

† Email address for correspondence: ishugan@yahoo.com

mathematical model of the sea surface imaging and establish mechanisms of surface wave perturbation by IWs.

The following basic properties of sea surface anomalies have been observed during combined oceanographic missions as a result of the interaction between IWs and sea surface waves (see Hughes & Grant 1978; Basovich, Bachanov & Talanov 1987; Gasparovic, Apel & Kasischke 1988):

(i) Wide bands of slicks and rough sea moving at the phase velocity of the IW train. These bands are most obvious at moderate and light wind speeds (lower than 5 m s^{-1}); as the wind strengthens, the width of the bands decreases appreciably.

(ii) The maximum modulation is observed in the context of co-propagation of sea wind waves and IWs. This is especially true for spectral components whose group velocity c_g is close to the IW phase velocity C ($c_g \sim C$); this condition is usually satisfied for short (of metre or decimetre lengths) gravity waves.

(iii) The entire interaction region is characterized by a smaller root mean square surface slope compared with the unperturbed surface: smooth surface regions occupy a greater area than do the rougher regions.

(iv) An individual slick cannot be uniquely mapped to the IW phase. It can be both above the IW trough and above the IW crest.

(v) The distance between the bands usually corresponds to the IW length.

The interaction between surface and internal waves has been studied both theoretically and experimentally over the last three decades.

A basic modulation mechanism for SW ranges of meter and decimeter lengths involves the hydrodynamic impact of a subsurface current induced by IWs on SWs (see Lewis *et al.* 1974; Phillips 1977). The quasi-steady model of such an impact on a linear surface wave packet was first proposed by Gargett & Hughes (1972) and Phillips (1977). Analysis of the relevant modulation equations confirmed that those packets with a group velocity approaching the IW phase velocity were most sensitive to subsurface currents. The SW amplitude in the group resonance range would grow infinitely, showing inapplicability of the developed linear modulation model to quantitatively describe the wave interactions.

Hughes (1978) proposed a consistent theory of IW action on linear surface gravity waves based on an equation for wave action that took into account the source and saturation terms of wind action on surface waves. The theory was consistent with observations of the modulation amplitude. No stationary solution was obtained for the relevant periodic processes, and as a consequence, the importance of group synchronism was demonstrated.

Recently the unsteady propagation of short surface waves in the presence of IW currents was studied by Donato *et al.* (1999) and Stocker and Peregrine (1999) using both simple ray theory for linear waves and a fully nonlinear numerical potential solver. Using ray theory, the researchers were able to explain the occurrence of focusing and they demonstrated that in such regions the waves steepened and could break. Comparisons were made between ray theory and the more accurate numerical simulations.

The effect of SW nonlinearity in the context of interaction with a slowly varying stationary current has also been analysed. Self-action of surface Stokes waves was shown by Holliday (1973) to lift the singularity of the resonant solution describing the SW dynamics in the context of a non-uniform current.

Smith (1976) derived the nonlinear Schrödinger equation that describes the local behaviour of reflecting surface waves by the stationary opposite current in the zone that is close to the blockage line. His work demonstrated the stability of the

stationary solutions. Today's challenge is to determine the interaction between surface and internal waves in cases where the resonant interaction regime is not local but can be treated as global. In such a scenario, every point in the region of interaction can be thought of as a 'blockage' point, surface and internal waves are coupled and the relative surface wave action flux equals zero. The nonlinear Schrödinger equation proposed in this paper describes the SW resonant modulation for the entire IW impact region.

Stokes wave stability was studied by Gerber (1987) for a non-uniform moving medium. An analogue of the third-order nonlinear Schrödinger equation was proposed for a complex envelope of the narrow-band wave packet. The carrier frequency behaviour in this scenario was determined using linear theory. The preferred approach allowed for the calculation of SW train dynamics under conditions far from resonance.

In spite of a significant amount of prior work, a thorough understanding of the relationship between IW characteristics and SW modulation across different length ranges is still lacking. We still have no exhaustive theoretical description of a number of important features related to SW and IW interaction that have been observed in various field investigations:

(i) *Forerunner of internal waves.* A significant number of experiments (see Basovich *et al.* 1987; Bakhanov *et al.* 1994) demonstrated surface wave anomalies at an extended distance (about 1 km) from the regions where internal waves exist, that is IW forerunner arises. Significant sea surface anomalies can be observed ahead of an IW train. These are much more obvious for a periodic train of linear IWs than for nonlinear quasi-solitary waves; the forerunner is not detected in some observations.

(ii) *Resonant excitation of surface waves.* Observations of resonantly coupled surface wave packets whose group velocity corresponds to the IW phase velocity in the absence of appreciable wind waves are discussed by Osborne & Burch (1980) and Phillips (1974). The IW observability at the sea surface seems to be very important. Of particular significance are localized wave solutions, in which the surface wave packets accompany the IWs and exponentially attenuate outside the region of interaction. The 'lifetime' of such wave formations under very noisy natural conditions should substantially exceed the characteristic time of interaction between wave packets of different velocities.

(iii) *Observations of strong internal waves on the sea surface.* Transformation of gravity capillary surface waves onto the current created by a large-amplitude internal wave was observed by Kropfli *et al.* (1999) and Bakhanov & Ostrovski (2002). In particular, the researchers studied the locations of the maxima and minima of the surface wave spectral density with respect to the IW profile. They demonstrated that for sufficiently large-amplitude internal solitary waves (solitons) propagating in the same direction as the surface wave the minimum density for all SW lengths is situated over the crest of the soliton. These field observations conflict with the theoretical expectation that the highest surface roughness would be near the region of the greatest surface gradient (see Gasparovic *et al.* 1988; Hogan *et al.* 1996). It should be noted, however, that the aforementioned conclusions were derived for sufficiently small IW currents, 1–2 cm s^{-1}, whereas in other cases currents may be many times larger for high-amplitude IW. This fact clearly emphasizes the importance of the wave's nonlinearity in the modelling IW effects at the sea surface.

(iv) *No uniformity in SW space modulations.* Spectral density variations may have a characteristic period that is shorter than that of periodic IWs (see Basovich *et al.* 1987; Bakhanov *et al.* 1994). The SW spectral density along a uniform periodic IW train grows on average from the train's end to its head; the spectral density of

decimetre-length SWs at the train head can exceed several times the unperturbed value. This in turn is significantly greater than the typical density associated with the opposing interaction in which the SWs are quasi-uniform along the IW train.

The goal of our work is to theoretically describe the aforementioned experimentally observed effects using a nonlinear SW modulation wave model. SW generation in the IW field can also be analysed by incorporating higher-order dispersion into the surface wave description. A uniformly valid steady model of the IW interaction with nonlinear Stokes surface waves, including the deep SW amplitude–frequency modulation, will be considered under conditions that approach the group resonance point. Such a model can be constructed by making allowance for the SW nonlinear dispersive properties that inevitably are linked with the impact of amplitude variations on the SW frequency in an inhomogeneous medium. An analysis of quasi-resonant conditions, under which SWs are strongly modulated by the IW train, allows us to establish quantitative parameters associated with the interaction. We approach the problem using the adiabatic approximation that does not include energy sources and sinks caused, for example, by wind and viscosity. This allows a pure representation of the role of nonlinearity when describing some fundamentally new observed experimental effects.

This paper consists of six sections. General equations that describe the one-dimensional interaction between an SW train and a non-uniform current induced by IWs are presented in § 2. Section 3 is dedicated to an analysis of the travelling solution for the resonant interaction scenario. Data on analytically and numerically calculated interactions for various types of IWs and initial SW parameters are presented in § 4. The model of parametrically resonant SW excited by internal waves is presented in § 5. Section 6 summarizes our final conclusions and discussion. Mathematical details of the asymptotic analytical solutions are presented in the Appendix.

2. Modulational equations of a one-dimensional interaction

The impact of IWs on the sea surface wave field is most significant for wave components with energy transport (group) velocities close to the IW phase velocity (see Gargett & Hughes 1972; Phillips 1977). Typical IW velocities (lower than 1 m s^{-1}) and lengths (no shorter than 150–200 m) under conditions close to the group resonance correspond to metre-length SWs. Hence, about 100 SW lengths and more can be settled within one IW length. Thus, the interacting waves have very different scales. Therefore, our problem can be considered as SW propagation in a slowly varying moving medium. The first set of complete equations to describe short waves propagating over much larger non-uniform currents was derived by Longuet-Higgins & Stewart (1964). Wave energy is not conserved and the concept of 'radiation stress' was introduced to describe the averaged momentum flux terms which govern the interchange of momentum with current. In our model, it is also sufficient to consider energy exchange in terms of the second-order wave action conservation law and neglect the effect of momentum transfer on the form of the surface current because it will be an effect only of the highest order (Stocker & Peregrine 1999).

We constructed our model of IW effects on the propagation of narrow-band weakly nonlinear Stokes packets of gravity SWs based on the following assumptions:

(i) Surface and internal waves propagate along a common x-direction.

(ii) The characteristic SW length $2\pi/k$ for wavenumber k is much shorter than the IW length $2\pi/K$, $K/k \ll 1$.

(iii) The depth of an oceanic pycnocline or a layer of maximum background current shear substantially exceeds the SW length, thus the IW in the upper layer of

a homogeneous (by density) fluid is calculated using a horizontal current that varies along the x-axis and reproduces the IW shape.

(iv) Vertical displacement of particles has a negligible impact on IW surface manifestations (Phillips 1977).

(v) Long IWs disperse weakly, and therefore the horizontal velocity of the current in the subsurface layer can be expressed as the travelling wave $U = U(K\xi) = U(K(x - Ct))$, where C is the phase velocity of IW propagation and $\xi = x - Ct$ is the associated coordinate.

(vi) We'll define horizontal subsurface current $U(K\xi)$, induced by the internal wave, through velocity potential: $\Phi_0(K\xi) : \mathrm{d}\Phi_0(K\xi)/\mathrm{d}\xi = U(K\xi)$. Fluid motion is accepted to be the potential since the horizontal current varies slowly enough, with $U_\xi/kU = O(\varepsilon^2)$, a_0 is a characteristic free-surface displacement, $2\pi/k_0$ is a typical surface wavelength and $\varepsilon = a_0 k_0 \ll 1$ is the conventional small average wave steepness parameter. The ratio U/C is assumed to be small, $U/C \sim \varepsilon$ which is usually confirmed by experimental data ($U/C \sim 0.1 - 0.3$) (see Hughes & Grant 1978; Gasparovic *et al.* 1988). This, along with the assumption $C \sim c_p/2$ (where c_p is the SW phase velocity), satisfies the continuity equation in the second order. Ultimately, the velocity potential function will be represented as a sum of the wave potential and the current potential $\phi(x, z, t) + \Phi_0(K\xi)$.

We wish to consider the set of equations for potential motion of an ideal incompressible infinite-depth fluid with a free surface given by the Laplace equation as follows:

$$\phi_{xx} + \phi_{zz} = 0, \quad -\infty < z < \eta(x, t); \tag{2.1}$$

the boundary conditions at the free surface:

$$g\eta + \phi_t + \frac{1}{2}\left(\phi_x^2 + \phi_z^2\right) = 0, \quad z = \eta(x, t), \tag{2.2}$$

$$\eta_t + \phi_x \eta_x = \phi_z, \quad z = \eta(x, t); \tag{2.3}$$

and at the bottom:

$$\phi = 0, \quad z = -\infty. \tag{2.4}$$

Here, $\eta(x, t)$ is the free-surface displacement, g is the acceleration due to gravity and t is time.

The variables are normalized as follows:

$$\left.\begin{aligned} &\phi = a_0\sqrt{\tfrac{g}{k_0}}\phi' = \varepsilon\sqrt{\tfrac{g}{k_0^3}}\phi', \quad \eta = a_0\eta' = \tfrac{\varepsilon}{k_0}\eta', \quad t = \tfrac{1}{\sqrt{gk_0}}t', \quad z = \tfrac{z'}{k_0}, \quad x = \tfrac{x'}{k_0}, \\ &U(K(x - Ct)) = U'(K/k_0(x' - C/c_p t'))c_p = U'(\varepsilon_1(x' - c't'))c_p, \end{aligned}\right\} \tag{2.5}$$

where $\varepsilon_1 = K/k_0$, another small parameter characterizing the ratio of the surface and internal wavelengths. We note that normalization (2.5) explicitly specifies the principal scales of the functions that we wish to characterize, namely $\phi = O(\varepsilon)$ and $\eta = O(\varepsilon)$. Then, the set (2.1)–(2.4) is reduced to the form

$$\phi_{xx} + \phi_{zz} = 0, \quad -\infty < z < \varepsilon\eta(x, t), \tag{2.6}$$

$$-\eta = \phi_t + U\phi_x + \varepsilon\tfrac{1}{2}\left(\phi_x^2 + \phi_z^2\right), \quad z = \varepsilon\eta(x, t), \tag{2.7}$$

$$\eta_t + U\eta_x + \varepsilon\phi_x\eta_x = \phi_z, \quad z = \varepsilon\eta(x, t), \tag{2.8}$$

$$\phi = 0, \quad z = -\infty, \tag{2.9}$$

where the primes are omitted. The weakly nonlinear surface wavetrain is described by a solution to (2.6)–(2.9), expanded into a Stokes series in terms of the small parameter ε.

Assuming the wave motion phase $\theta = \theta(x, t)$ in the presence of a slowly varying current U, we define the local wavenumber k and frequency σ as

$$k = \theta_x, \quad \sigma + kU = -\theta_t. \tag{2.10}$$

These primary wave parameters together with the first-order velocity potential amplitude ϕ_0 will be considered further to be slowly varying on a typical scale of $O(\varepsilon^{-1})$. This is longer than the primary wavelength and period (Whitham 1974):

$$\phi_0 = \phi_0(\varepsilon x, \varepsilon t), \quad k = k(\varepsilon x, \varepsilon t), \quad \sigma = \sigma(\varepsilon x, \varepsilon t). \tag{2.11}$$

Using this framework, we wish to recover the effects of long-scaled current and nonlinear wave dispersion. These effects are additive (since they have the same order) with the Stokes term, since they reflect the square of the wave steepness.

The solution to the problem, uniformly valid to $O(\varepsilon^3)$, is found by a two-scale expansion with the differentiation

$$\frac{\partial}{\partial t} = -(\sigma + kU)\frac{\partial}{\partial \theta} + \varepsilon \frac{\partial}{\partial T}, \quad \frac{\partial}{\partial x} = k\frac{\partial}{\partial \theta} + \varepsilon \frac{\partial}{\partial X}, \quad T = \varepsilon t, \quad X = \varepsilon x. \tag{2.12}$$

Substitution of the velocity potential in its linear form, $\phi = \phi_0 e^{kz} \sin\theta$, satisfies the Laplace equation (2.6) in the first order in ε due to (2.10) and gives the following additional terms in the second order $O(\varepsilon^2)$:

$$\varepsilon(2k\phi_{0X} + k_X\phi_0 + 2kk_X\phi_0 z)\mathrm{e}^{kz}\cos\theta + \cdots = 0. \tag{2.13}$$

To satisfy the Laplace equation in the second order, Yuen & Lake (1982) and Shugan & Voliak (1998) suggested an additional phase-shifted term with a linear and quadratic z correction in the representation of the potential function ϕ:

$$\phi = \phi_0 \mathrm{e}^{kz}\sin\theta - \varepsilon\left(\phi_{0X} z + \frac{k_X\phi_0}{2}z^2\right)\mathrm{e}^{kz}\cos\theta + \cdots. \tag{2.14}$$

Exponential decay of the wave's amplitude with z is accompanied by a second-order subsurface jet due to slow horizontal variations of the wavenumber and amplitude of the wave packet.

The free-surface displacement $\eta = \eta(x, t)$ is also expressed as an asymptotic series,

$$\eta = \eta_0 + \varepsilon\eta_1 + \varepsilon^2\eta_2 + \cdots, \tag{2.15}$$

where η_0, η_1 and η_2 are $O(1)$ functions that we wish to determine. Using expressions (2.14)–(2.15) subject to the dynamic boundary condition (2.7), we consequently find the components of the free-surface displacement as follows:

$$\eta_0 = \sigma\phi_0\cos\theta, \tag{2.16}$$

$$\eta_1 = -\phi_{0T}\sin\theta - U\phi_{0X}\sin\theta + \frac{1}{2}\sigma^2 k\phi_0^2\cos(2\theta), \tag{2.17}$$

$$\eta_2 = -\frac{3}{8}\sigma k^3\phi_0^3\cos\theta. \tag{2.18}$$

Only the self-action term with fundamental wave phase θ is included in the third-order displacement (2.18).

Substitution of velocity potential (2.14) and displacement (2.15)–(2.18) into the kinematics boundary condition (2.8) gives the following relationships between the

wave modulation characteristics:

$$\sigma^2 = k + \varepsilon^2 k^4 \phi_0^2 + \varepsilon^2 (\phi_{0TT} + 2U\phi_{0XT} + U^2 \phi_{0XX})/\phi_0, \tag{2.19}$$

$$\left[\phi_0^2 \sigma\right]_T + \left[\left(U + \frac{1}{2\sigma}\right)\phi_0^2 \sigma\right]_X = 0. \tag{2.20}$$

The first of these formulas represents the wave dispersion relation with the total second-order amplitude-phase dispersion included in the presence of the current U. Equation (2.20) yields the known wave action conservation law. Modulation equations (2.19)–(2.20) are closed by the equation of wave phase conservation that follows from (2.10) as a compatibility condition (Phillips 1977):

$$k_T + (\sigma + kU)_X = 0. \tag{2.21}$$

The derived set of equations (2.19)–(2.21) in the absence of a current coincides with those of Shugan & Voliak (1998).

3. Travelling wave solution

We wish to analyse the travelling wave solutions to the problem (2.19)–(2.21) under the assumption that all the unknown functions depend on the single coordinate $\xi = X - cT$, such that all the waves are stationary. Then, after integrating (2.20) and (2.21), the problem is of the form

$$\sigma^2 = k + \varepsilon^2 k^4 \phi_0^2 + \varepsilon^2 (U(\xi) - c)^2 \phi_{0\xi\xi}/\phi_0, \tag{3.1}$$

$$(U(\xi) - c + c_g)\phi_0^2 \sigma = A, \tag{3.2}$$

$$\sigma + k(U(\xi) - c) = \Omega, \tag{3.3}$$

where $c_g = 1/(2\sigma)$ is the linear group velocity of the surface waves, and A and Ω are the integration free constants with the physical meaning of wave action flux and frequency, respectively, measured in the moving coordinate frame. The values of constants are determined from the boundary conditions for the uniform Stokes wave at infinity. In the dimensional form, these values are

$$A = \left(\frac{1}{2}\sqrt{\frac{g}{k_0}} - C\right)\frac{a_0^2}{\sqrt{gk_0}}; \quad \Omega = \sqrt{gk_0}\left(1 + \frac{1}{2}(a_0 k_0)^2\right) - k_0 C,$$

where a_0, k_0 are the constant amplitude and wavenumber of the Stokes wave in the absence of current at infinity.

The analysis of the linear problem (see Gargett & Hughes 1972; Lewis *et al.* 1974) where the dispersion relation (3.1) is independent of the SW amplitude satisfactorily describes the wave modulation under conditions far from the group resonance $c \approx c_g$. Amplitude distribution can be found from the energy equation (3.2) after solving the 'kinematic' closed set of equations (3.1) and (3.3) for the wavenumber and frequency. In the resonance vicinity

$$U(\xi) - c + c_g = 0, \tag{3.4}$$

the solution found has singularities consistent with an infinite amplitude growth at the points of SW 'blockage' by the current (see (3.2)). This in turn defines a 'barrier' for SW propagation. In this case, the linear steady solution becomes incorrect.

After eliminating the wavenumber k and frequency σ the set (3.1)–(3.3) transforms into a single equation for the first-order potential amplitude ϕ_0:

$$\frac{1}{(U-c)^2}\left(\frac{A}{\phi_0^2}\right)^2 = \frac{(1+4\Omega(U-c))}{4(U-c)^2} + \varepsilon^2\left(\left(\frac{1}{2}-\frac{A}{\phi_0^2}\right)\frac{1}{(U-c)^2}+\frac{\Omega}{(U-c)}\right)^4 \times \phi_0^2 + \varepsilon^2(U-c)^2\phi_{0\xi\xi}/\phi_0. \tag{3.5}$$

The main feature of the model is clearly visible from (3.5): the solution in the zero order on ε exists for positive values of the expression

$$1+4\Omega(U(\xi)-c), \tag{3.6}$$

depending only on the flow velocity and on the basic parameters of the problem. For sufficiently large negative values of $U(\xi)$, expression (3.6) can become equal to zero or even negative. Accordingly the highest orders of the dispersion relation then have to be taken into account. It can be shown that the zero value of expression (3.6) corresponds to the condition of zero local velocity of wave action flux and as a result, this is linked to unlimited growth of the wave amplitude (see (3.2)).

4. Stokes surface wave, resonantly modulated by the current

First we wish to analyse the derived set (3.1)–(3.3) under the resonant boundary conditions (3.4). At $A = 0$ the energy equation immediately yields the following result: the SW energy flux through any section $\xi = \xi_0$ is zero in the frame of reference that is consistent with the IWs. The aforementioned blockage condition (3.4) defines the direct modulation of the surface wavenumber by the current

$$k = k_0\left(1+\frac{3U(\xi)}{c}\right). \tag{4.1}$$

Hence, the SW length in the resonant interaction mode is modulated rather weakly by the current induced by IWs. In this case, the SWs shorten and lengthen respectively at down- and countercurrents.

Modulation of an initially homogeneous Stokes wave will be considered under the following boundary conditions:

$$\xi \to -\infty, \quad U(\xi) \to 0, \quad \phi_0 \to 1, \quad k \to 1. \tag{4.2}$$

Free parameters in the set (3.1)–(3.3) can be determined using the boundary condition (4.2):

$$c = \frac{1}{2}-\frac{\varepsilon^2}{4}; \quad \Omega = \frac{1}{2}+\frac{3\varepsilon^2}{4}. \tag{4.3}$$

We note that no dimensional value of the velocity $c = 1/2$ corresponds to a leading order of the linear group velocity of surface waves. Due to the condition of phase synchronism, there is also mapping to the phase velocity of the internal wave.

Equation (3.5) up to $O(\varepsilon^2 U/c, \varepsilon_1^2 U/c)$ takes the form

$$G_2\phi_{0\xi'\xi'} + (G_0 u(\xi')-1)\phi_0 + \phi_0^3 = 0, \tag{4.4}$$

where ξ' is the renormalized variable in the context of the IW space scale ($\xi' = (\varepsilon_1/\varepsilon)\xi$ and primes can be omitted), $u(\xi) = U(\xi)/|U_0|$ is the current velocity function, normalized by its maximum amplitude, while

$$G_2 = \left(\frac{K}{2k_0}\right)^2\frac{1}{(a_0k_0)^2}$$

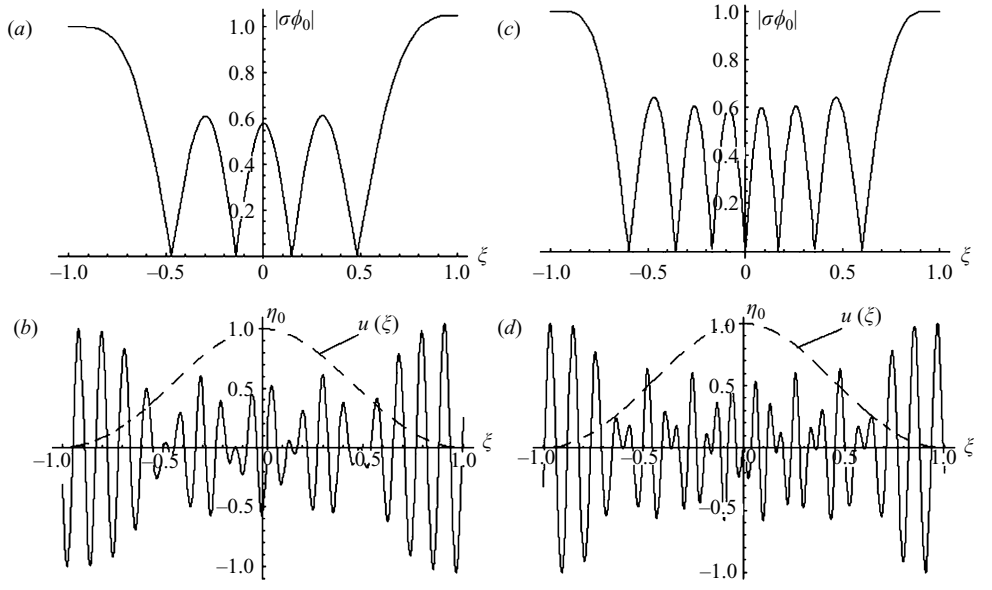

FIGURE 1. Surface elevation envelope $\sigma\phi_0 = \sigma\phi_0(\xi)$ and first harmonic of the surface profile $\eta_0(\xi)$ on the downcurrent $u(\xi) = (\sec\mathrm{h}\,(x) - \sec\mathrm{h}\,(1))^2/(\sec\mathrm{h}\,(0) - \sec\mathrm{h}\,(1))^2$ for $c = 0.5$, $\varepsilon = 0.1$, $G_2 = 0.05$; (*a, b*) $G_0 = 7$, (*c, d*) $G_0 = 18$; the dashed curve is the current profile $u(\xi)$.

is the relationship between surface and internal typical wavelengths and SW initial steepness $G_0 = \frac{2|U_0/c_p|}{(a_0k_0)^2} \sim O(\varepsilon^{-1})$ is a large parameter which characterizes the value of subsurface current relative to the unperturbed SW steepness.

Equation (4.4), subject to the boundary conditions (4.2), was analysed analytically and numerically for various values of the controlling dimensionless parameters G_0 and G_2. The current velocity function $u(\xi)$ is presented in (4.4) in its normalized form (both space and amplitude scales are represented in the dimensionless parameters G_0 and G_2). Therefore, in analytical simulations, we wish to assume that function $u(\xi)$ is a solitary-type smooth function with a non-zero value within the interval $(-1, 1)$ and a maximal amplitude that is equal to the unit. Our asymptotic analysis is based on the method of multiscale expansions for the nonlinear ordinary second-order differential equations with slowly varying coefficients (see Kuzmak 1959; Luke 1966). Details of the asymptotic solution are presented in the Appendix.

We first consider the data calculated for the modulation of SW by the typical solitary type IW positive current $u(\xi) = (\sec\mathrm{h}(x) - \sec\mathrm{h}(1))^2/(\sec\mathrm{h}(0) - \sec\mathrm{h}(1))^2$ for the near-resonant conditions of wave interaction. The results of numerical calculations for the exact resonance case ($A = 0$) are shown in figure 1 for two different values of the current intensity parameter G_0. The SW envelope is presented together with the profile of the lowest harmonic $\eta_0 = \sigma\phi_0 \cos\theta$ of the sea surface displacement. The analytical solution to the problem conforms well to numerical calculations. Here, the basic effect is a deep wave modulation regime presented as a strong smoothing of the sea surface over the developed current. The decreasing wave amplitude is accompanied by the formation of several zero-level minima, the number of which grows with the intensity of the IW-induced current. As the interaction length grows (G_2 decreases), the smoothing strengthens.

We also performed numerical simulations of the SW modulation by IW-induced currents for various ranges of SW frequencies on the basis of the general modulation

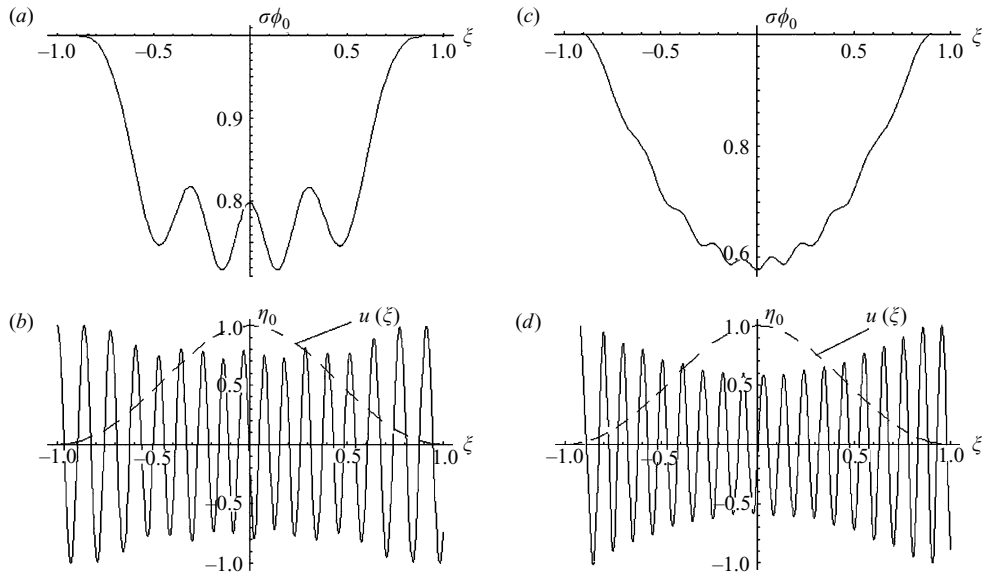

FIGURE 2. Surface elevation envelope $\sigma\phi_0 = \sigma\phi_0(\xi)$ and first harmonic of the surface profile $\eta_0(\xi)$ on the downcurrent $u(\xi) = (\sec\mathrm{h}\,(x) - \sec\mathrm{h}\,(1))^2/(\sec\mathrm{h}\,(0) - \sec\mathrm{h}\,(1))^2$ for $\varepsilon = 0.1$, $G_2 = 0.05$, $G_0 = 7$; (*a, b*) $c = 0.55$, (*c, d*) $c = 0.45$; the dashed curve is the current profile $u(\xi)$.

equation (3.5). Typical examples of our numerical calculations for the general equation (3.5) are presented in figure 2 for the cases of the relatively long ($c < 1/2$) and short ($c > 1/2$) SW. It is clear from figure 2 that the wave system is modulated in a regular measured manner; this is substantially different from the resonant behaviour. Our results clearly show that the most aggressive modulations take place for the SWs in the vicinity of resonance conditions ($c \sim 1/2$) and sharply decrease far from the group resonance frequencies.

Numerical calculations of SW variation for the near-resonant conditions at the negative current $u(\xi) = -(\sec\mathrm{h}(x) - \sec\mathrm{h}(1))^2/(\sec\mathrm{h}(0) - \sec\mathrm{h}(1))^2$ are shown in figure 3 for two different intensities of the IW-induced current G_0. The asymptotic solution (see Appendix) describes the basic properties of SW modulation satisfactorily. The main property of this solution is that the envelope of the SW in the context of counterflow may increase considerably, surpassing its initial value by a factor of several times. For sufficiently large-scale IW ($G_2 \leqslant 0.05$), the SW envelope reproduces the shape of the subsurface current. The modulation amplitude grows with the intensity of the IW-induced current and is symmetric relative to the current profile axis. Moreover, high-frequency modulation of the SW envelope grows as well.

The data for shorter IWs ($G_2 \geqslant 0.1$) and a slight mismatch from the resonance regime ($c < 1/2$) are shown in figure 4. The wave amplitude $\phi_0(\xi)\sigma(\xi)$ of the sea surface is presented together with the fundamental harmonic surface profile $\eta_0(\xi)$, instantaneous frequency $\sigma(\xi)$ and phase $\theta(\xi) = \varepsilon^{-1}\int \sigma/(c-u)\mathrm{d}\xi$. The following interaction features are noteworthy: the SW steepness modulation maximum shifts to the IW head slope as IW horizontal magnitude decreases. Another remarkable particularity of the solution is the IW forerunner: ahead of the IW, in the region with no current, an intensive periodic SW train propagates with low-frequency modulation exceeding the entering wave amplitude. Deep wave modulation is accompanied by the formation of anomalies in the surface profile with zero or even negative values of

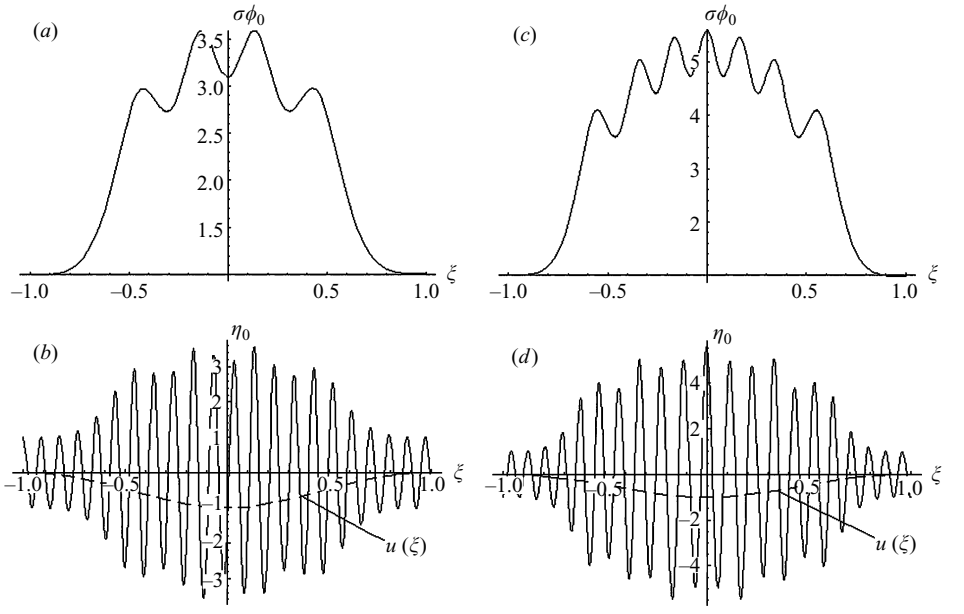

FIGURE 3. Surface elevation envelope $\sigma\phi_0 = \sigma\phi_0(\xi)$ and first harmonic of the surface profile $\eta_0(\xi)$ on the countercurrent $u(\xi) = -(\sec h(x) - \sec h(1))^2/(\sec h(0) - \sec h(1))^2$ for $c = 1/2$, $\varepsilon = 0.07$, $G_2 = 0.05$; (*a, b*) $G_0 = 12$, (*c, d*) $G_0 = 36$; the dashed curve is the current profile $u(\xi)$.

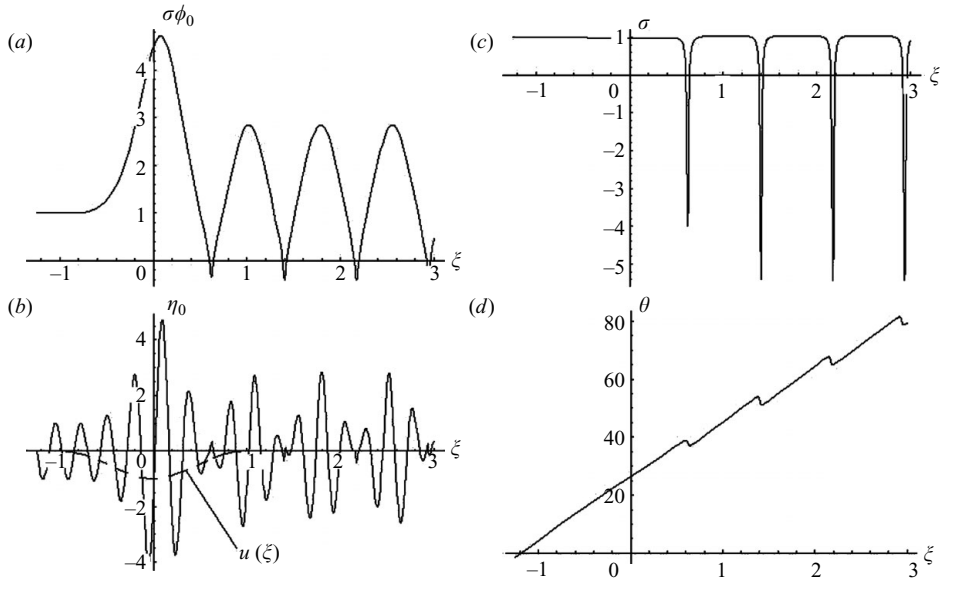

FIGURE 4. Surface elevation envelope $\sigma\phi_0 = \sigma\phi_0(\xi)$ (*a*), first harmonic of the surface profile $\eta_0(\xi)$ (*b*), wave frequency $\sigma(\xi)$ (*c*) and phase $\theta(\xi)$ (*d*) on the countercurrent $u(\xi) = -(\sec h(x) - \sec h(1))^2/(\sec h(0) - \sec h(1))^2$ for $c = 0.47$, $\varepsilon = 0.08$, $G_2 = 0.4$, $G_0 = -10$; the dashed curve is the current profile $u(\xi)$.

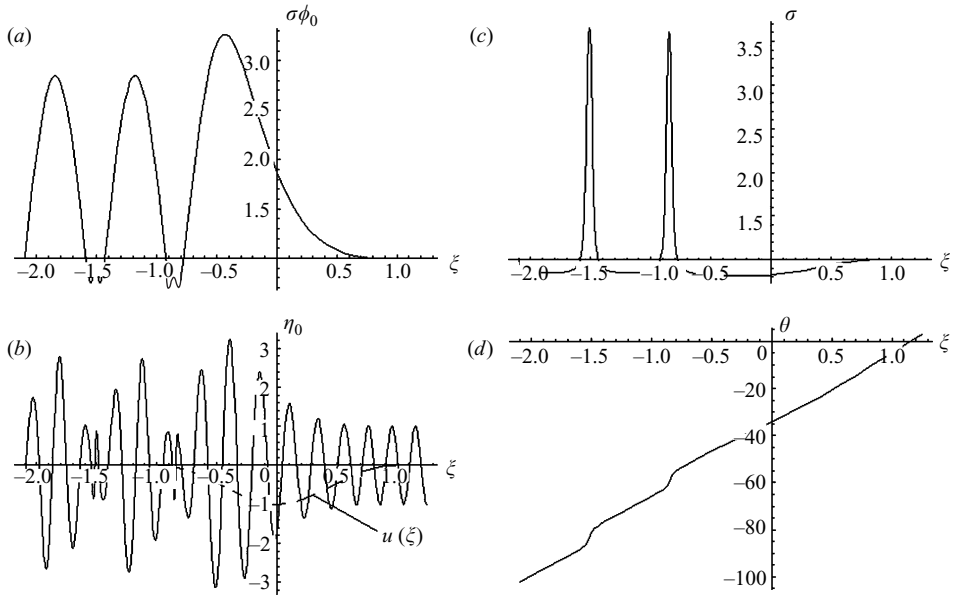

FIGURE 5. Surface elevation envelope $\sigma\phi_0 = \sigma\phi_0(\xi)$ (*a*), first harmonic of the surface profile $\eta_0(\xi)$ (*b*), wave frequency $\sigma(\xi)$ (*c*) and phase $\theta(\xi)$ (*d*) on the countercurrent $u(\xi) = -(\sec\mathrm{h}\,(x) - \sec\mathrm{h}\,(1))^2/(\sec\mathrm{h}\,(0) - \sec\mathrm{h}\,(1))^2$ for $c = 0.6$, $\varepsilon = 0.07$, $G_2 = 0.25$, $G_0 = -15$; the dashed curve is the current profile $u(\xi)$.

wave amplitude (figures 4*a* and 4*b*). The frequency $\sigma(\xi)$ (figure 4*c*) sharply drops in these locations to large negative values, while the phase $\theta(\xi)$ (figure 4*d*) runs in the opposite direction and has sharp kinks exactly co-localized with the minimum surface elevations. A solution of this type has all the key characteristics of the phase reversals or 'crest pairing' observed by Melville (1983) and Chereskin & Mollo-Cristensen (1985) and described by Shugan & Volyak (1998).

This means that the relatively long SW ($c < 1/2$), after crossing the region of internal wave current, maintains its deep low-frequency amplitude modulations with local surface smoothing and phase reversals. That property is confirmed by field measurements (Basovich *et al.* 1987; Bakhanov *et al.* 1994).

Figure 5 shows the scenario in which the IW crosses the field of short SW ($c > 1/2$), resulting in SW low-frequency modulations. The intensity of modulations in the trace of the IW is comparable to the primary peak modulations. One can also see certain spikes in surface wave amplitude (figures 5*a* and 5*b*) synchronous with the sharp positive impulses of instantaneous frequency $\sigma(\xi)$ (figure 5*c*) and rapid jumps in the phase $\theta(\xi)$ (figure 5*d*).

The opposite 'polarity' of the peculiarities of the forerunner ($c < 1/2$) and trace ($c > 1/2$) waves is defined by the sign of the wave action flux A, which is positive for a long SW moving faster than IW and negative for a relatively short and slow SW. The expression for the wave frequency, following from the wave action conservation equation (3.2), has the form

$$\sigma = \frac{\phi_0^2 - 2A}{2\phi_0^2(c-u)}.$$

From the above expression it is evident that for vanishing amplitudes of the velocity potential $\phi_0^2 \to 0$ and positive wave flux $A > 0$ the frequency may drop sharply, even reaching large negative values where it may lead to phase reversals. For a negative

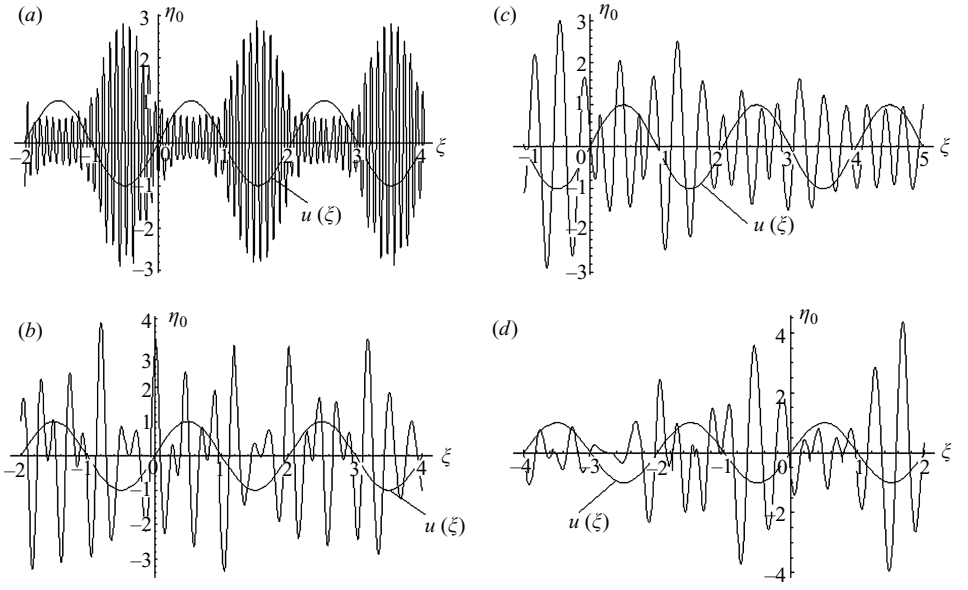

FIGURE 6. First harmonic of the surface profile $\eta_0(\xi)$ on the periodic current $u(\xi) = \sin(\pi\xi)$ for (*a*) $c = 0.44$, $\varepsilon = 0.12$, $G_2 = 0.02$, $G_0 = 7$; (*b*) $c = 0.5$, $\varepsilon = 0.1$, $G_2 = 0.3$, $G_0 = 5$; (*c*) $c = 0.6$, $\varepsilon = 0.07$, $G_2 = 0.35$, $G_0 = 8$; (*d*) $c = 0.48$, $\varepsilon = 0.13$, $G_2 = 0.2$, $G_0 = 10$; the dashed curve is the current profile $u(\xi)$.

wave flux $A < 0$ a positive frequency impulse will be evidenced together with a positive phase jump.

A significant forerunner or trace of the IW will be seen only in the context of a negative counterflow and does not appear for a positive subsurface current.

To explain a number of described wave modulation phenomena, we wish to consider the data describing the impact of the periodic subsurface current $u(\xi) = \sin(\pi\xi)$ on the initially uniform Stokes surface wavetrain. Figure 6 shows the most interesting regimes of surface displacement $\eta_0(\xi)$ variations for different SW frequencies, current space period and intensities as described by the set of model parameters $(G_0, G_2, \varepsilon, c)$.

The typical example of SW modulation caused by a sufficiently long IW ($G_2 = 0.02$) is presented in figure 6(*a*) for the following parameter values: $c = 0.45$, $\varepsilon = 0.12$, $G_0 = 7$. One observes a regular and periodic wave modulation behaviour which reproduces the periodic structure of the subsurface current. Surface amplitude increases many times in the countercurrent scenario and smoothes on the downcurrent.

The possibility of SW modulation in cases of length period shorter than that of the IW is shown in figure 6(*b*). This is the resonant regime of modulation ($c = 1/2$) by a short IW ($G_2 = 0.3$). The space period of SW modulation peaks is almost half that of the IW period.

The non-uniform regimes of modulation are shown in figures 6(*c*) and 6(*d*). Increasing amplitude variations from the front to the tail for the short period IW train ($G_2 = 0.35$) and short SW ($c = 0.6$) is shown in figure 6(*c*). The modulation instability of long SW ($c = 0.48$) while crossing the IW field is shown in figure 6(*d*).

The aforementioned modulation effects, including the SW amplitude variations with a characteristic period shorter than that of the periodic IW and the effects of amplitude growth from the tail to the front along the uniform periodic IW train, were experimentally observed by Bakhanov *et al.* (1994).

As a final point a few concluding remarks on the phase singularities solutions.

During the past few years, a great deal of attention has been paid to the structure of wave fields in the neighbourhood of points where the SW amplitude has zero value. Explicit solutions, the family of solitons on finite background, of the nonlinear Schrödinger equation for the modulated surface wavetrain were used to study phase singularities in detail by Karjanto & van Groesen (2007) and Andonovati, Karjanto & van Groesen (2007). It is shown that at singular points of a wave field, where amplitude vanishes, phase may become singular and wavefront dislocation may occur. Regrettably, the applicability of nonlinear Schrödinger equation weakly nonlinear model to describe the rapid variations of wavenumber and frequency in the phase singularities locations was not discussed in these papers.

The present model generalizes nonlinear Schrödinger equation theory, to which it transforms at certain values of the governing parameters. The model with deeply modulated wavenumber and frequency permits one also to analyse the appropriately short surface wave packets and modulation periods.

However we note that phase singularities and corresponding very rapid changing of wavenumber and frequency contradicts our initial assumption of slowly varying modulation parameters of the narrow-banded surface wavetrain. At the same time side phase jumps take place in very small locations with a wave amplitude close to zero and that is why asymptotic series of the solution (2.15)–(2.18) are still in order and not broken in these regions. Solution gives the fully recovering values of the wavenumber and frequency after crossing the phase singularity localizations. Experimental data confirm that the phase singularities appear at locations where the wave's amplitude vanishes. In conclusion we believe that presence of phase jumps does not break applicability of the present model to describe behaviour of deeply modulated SW trains.

5. Surface wave excitation by an internal wavetrain

One of the most intriguing and poorly understood phenomena are resonantly coupled surface wave packets whose group velocity corresponds to the IW phase velocity in the absence of appreciable wind waves (see Phillips 1974; Osborne & Burch 1980).

Wave self-action theory allows for the expansion of the scope of the described IW manifestations at the sea surface. We consider the problem of wave resonant excitation in the field of an IW-induced current. We wish to search for non-trivial solutions to the set of interaction equations (3.1)–(3.3) with zero boundary conditions

$$\phi_0 \to 0 \quad as \quad u(\xi) \to 0\,, \quad \xi \to \pm\infty\,. \tag{5.1}$$

These conditions yield a zero value for the wave action flux in the right-hand side of (3.2), that is $A = 0$. Accordingly, it immediately follows that SWs can be generated only when the group resonance conditions (3.4) are satisfied across the entire current region such that the group velocity of excited SWs to within $O(U/c)$ is equal to the SW phase velocity. Outside the current region, the surface wavenumber is constant, so it will be fixed as a typical value $k_0 = 1(\xi = -\infty)$. The free parameter in (3.3) can be determined by using the boundary condition (5.1): $\Omega = 1/(2c) - c$. Equation (3.5) for the velocity potential ϕ_0 with accuracy of up to $O(\varepsilon^2 U/c)$ takes the form

$$\phi'_{0\xi'\xi'} + G_I(u'(\xi') - \lambda)\phi'_0 + \phi'^3_0 = 0, \tag{5.2}$$

where $G_I = (gL/4\pi C^2)^2 \gg 1$ is the primary non-dimensional parameter for the boundary value problem that characterizes the internal waves (L and C are the length of the region occupied by the current and phase velocity of IW, respectively). ξ' is the

renormalized variable that describes the space scale of the IW $\xi' = (\varepsilon_1/\varepsilon)\xi$; $u' = 4\Omega u$; $\phi_0' = (\varepsilon/\varepsilon_1)\phi_0$; $\lambda = 1 - 4c^2$ and primes will be omitted hereafter.

The common approach to the asymptotic solution of (5.2) includes merging of the external soliton solution ϕ_{0e} which satisfies the zero boundary conditions (5.1) at infinity for the outside of the current region with the internal solution ϕ_{0i} for the interaction zone $(-1, 1)$. The details of the asymptotic analysis are presented in the Appendix.

The main property of the resulting solution is that the resonant coherent surface waves ($C \sim c_g$) may be effectively excited in the context of a counterflow scenario produced by IW and that reproduces the shape of the subsurface current. The resonant excitation of surface waves has the following dynamic threshold for the intensity of subsurface currents in the dimensional form

$$G_I^{1/2} \left(\frac{L}{2\sqrt{2}}\right)^{-1} \int_{-L/2}^{L/2} \left(-\frac{U(\xi)}{C}\right)^{1/2} \mathrm{d}\xi = 2\pi n,$$

where $n = 1, 2, 3, \ldots$ are arbitrary positive integers corresponding to the different modes of excited SW. This is consistent with the classical Bohr–Sommerfeld quantization rule in quantum mechanics (see Landau & Lifshitz 1977).

The amplitude of the generated SW grows with the intensity of the IW-induced current and is symmetric relative to the current profile axis.

The modelling of parametric exciting SW on the downcurrent ($U(\xi) > 0$) was achieved using an approach similar to that presented in § 4. Significant surface waves are not generated in this case, and they attenuate in the same manner as initially uniform Stokes waves on the downcurrent.

6. Conclusions

We were able to use our new nonlinear model of SW–IW interaction to describe a number of experimental effects that have been observed to date. These include the exposure of strong internal waves, forerunners of IW, resonant excitation of surface waves and non-uniformity of periodic IW exposure on the sea surface.

Our account of SW nonlinearity allows us to construct uniformly valid stationary solutions to the problem in the vicinity of group velocity resonance.

The basic properties of our solution are consistent with the results of observations of SW modulations by large amplitude internal waves (see Kropfli *et al.* 1999; Bakhanov & Ostrovski 2002), by relatively short internal waves (Basovich *et al.* 1987; Bakhanov 1994) and in resonant excitation of SW in the presence of IW (Phillips 1974; Osborne & Burch 1980).

We note the key results of our near-resonant SW modulation model:

(i) Interaction with large-scale solitary IWs leads to strong modulations of the SW envelope. The surface countercurrent causes a growth in SW steepness and results in an envelope shape that follows the current profile. The steepness of modulation grows with the intensity of IW-induced current and is symmetric relative to the current profile axis. A moderate high-frequency oscillation is imposed on the algebraic part of the solution.

(ii) Modulation by a large-scale positive solitary IW-induced current leads to surface smoothing accompanied by the formation of several zero-level amplitude minima, the number of which grows with the intensity of the IW-induced current. As the interaction length grows, the smoothing strengthens accordingly.

(iii) An IW forerunner can arise ahead of the IW train for a long SW, manifesting itself as a modulated SW train with a period that is comparable to the IW spatial scale. Leaving the internal wave field, the surface waves preserve the resulting modulation.

(iv) A trace of IW in the case of negative subsurface current can also arise for a relatively short SW scenario in the form of a modulated SW train of comparable intensity.

(v) The modulation period of surface waves can be shorter than the IW period (for short periodic and following IW trains) and the modulation depth may be non-uniform along the IW train.

(vi) Excitation of resonantly coupled surface wave packets whose group velocity corresponds to the IW phase velocity is effective on the counter subsurface flow produced by IW. It has a dynamic threshold that is defined by the space scale and intensity of the internal waves.

Appendix

A.1. An asymptotic solution of the equation (4.4)

Multiscale asymptotic techniques together with the method of merging the asymptotic expansions are used to construct the solutions to (4.4) and (5.1) for the resonant impact of subsurface current on SW propagation.

The transition of (4.4) with a big parameter G_0 to the equation with slowly varying coefficients can be made by introducing the slow and fast variables:

$$\Phi_{\eta\eta} + a(\xi)\Phi + \Phi^3 = 0, \tag{A 1}$$

where ξ and $\eta = \xi\sqrt{G_0/G_2}$ are slow and fast variables, respectively, and $\Phi = \phi_0/\sqrt{G_0}$, $a(\xi) = u(\xi) - 1/G_0$. We search for an almost periodic solution of (A 1) that is in the form

$$\Phi = \Phi(\omega, \xi), \tag{A 2}$$

where $\mathrm{d}\omega/\mathrm{d}\eta = \varphi(\xi)(\varphi(\xi)$ is the $O(1)$ slowly varying instantaneous frequency of oscillations to be determined).

Equation (A 1) when substituted into (A 2) results in

$$\varphi^2(\xi)\frac{\partial^2\Phi}{\partial\omega^2} + \frac{1}{\sqrt{G_0}}\left[2\varphi(\xi)\frac{\partial^2\Phi}{\partial\omega\,\partial\xi} + \varphi'(\xi)\frac{\partial\Phi}{\partial\omega}\right] + \frac{1}{G_0}\frac{\partial^2\Phi}{\partial\xi^2} + \Phi^3 + a(\xi)\Phi = 0. \tag{A 3}$$

Assuming the existence of a uniformly valid solution we write $\Phi(\omega, \xi)$ as

$$\Phi(\omega, \xi) = \Phi_0(\omega, \xi) + 1/\sqrt{G_0}\Phi_1(\omega, \xi) + O(1/G_0). \tag{A 4}$$

Substitution of (A 4) into (A 3) and subsequent expansion of the result in powers of $1/\sqrt{G_0}$ leads to equations of the first and second approximations, respectively,

$$\varphi^2(\xi)\frac{\partial^2\Phi_0}{\partial\omega^2} + \Phi_0^3 + a(\xi)\Phi_0 = 0, \tag{A 5}$$

$$\varphi^2(\xi)\frac{\partial^2\Phi_1}{\partial\omega^2} + \left[3\Phi_0^2 + a(\xi)\right]\Phi_1 = -2\varphi(\xi)\frac{\partial^2\Phi_0}{\partial\omega\partial\xi} - \varphi'(\xi)\frac{\partial\Phi_0}{\partial\omega}. \tag{A 6}$$

Equation (A 5) contains two unknown functions $\Phi_0(\omega, \xi)$ and $\varphi(\xi)$ that can be determined by studying (A 6) of the second approximation.

Kuzmak (1959) proved the theorem that if periodic solutions Φ_0 and Φ_1 with a period of ω independent of ξ can be found for (A 5) and (A 6), and then the error $O(1/G_0)$, within which (A 3) is satisfied, will be uniformly bounded.

The condition of function Φ_1 periodicity is given by Kuzmak (1959)

$$\varphi(\xi)\int_{a_1}^{a_2}\left(\frac{\partial\Phi_0}{\partial\omega}\right)^2\mathrm{d}\omega = D, \tag{A 7}$$

where D is constant and a_1 and a_2 are sequential zeros of the derivative $\partial\Phi_0/\partial\omega$.

Since the terms of order $(1/\sqrt{G_0})$ in (A 4) represent small oscillating corrections to the principal terms, one can usually neglect those terms that involve $(1/\sqrt{G_0})$. Thus, the asymptotic formulas for the solution of (A 3) and its derivative have the form

$$\Phi_0(\xi) = \Phi_0(\omega(\eta), \xi), \left(\frac{\partial \Phi_0}{\partial \eta}\right)_0 = \varphi(\xi)\frac{\partial \Phi_0}{\partial \omega},$$
$$\left(\eta = \sqrt{G_0/G_2}\xi, \omega = \omega_0 + \int_{\eta_0}^{\eta} \varphi(\eta/\sqrt{G_2/G_0})\mathrm{d}\eta\right).$$

Therefore, to determine an asymptotic solution it is necessary to solve a system consisting of (A 5) and of the condition of periodicity (A 7).

Boundary conditions for initially homogeneous Stokes waves at $\xi = -1$ are

$$\Phi_0(-1) = 1/\sqrt{G_0}; \quad \Phi_{0\xi}(-1) = 0. \tag{A 8}$$

We shall seek an approximate solution of the form

$$\Phi_0(\omega, \xi) = \sum_{n=0}^{N} B_n(\xi)\cos(n\omega). \tag{A 9}$$

Substituting (A 9) into (A 5), equating to zero the coefficients of similar harmonics and neglecting harmonics higher than N in the case when $N = 1$, we obtain

$$\left.\begin{aligned} a(\xi)B_0(\xi) + B_0(\xi)\left[B_0^2(\xi) + 3/2B_1^2(\xi)\right] = 0; \\ -\varphi^2(\xi)B_1(\xi) + a(\xi)B_1(\xi) + B_1(\xi)\left[3B_0^2(\xi) + 3/4B_1^2(\xi)\right] = 0. \end{aligned}\right\} \tag{A 10}$$

This system consists of two equations and three unknowns: $B_0(\xi)$, $B_1(\xi)$, $\varphi(\xi)$. The required additional equation is obtained by substituting (A 9) into the condition of periodicity (A 7):

$$\varphi(\xi)B_1^2(\xi) = D; \tag{A 11}$$

here D is an arbitrary constant to be determined from the boundary conditions.

We first consider the modulation of SW on a downflow when $a(\xi) > 0$. The system of (A 10)–(A 11), thanks to $a(\xi)$ being positive, can be reduced to

$$\left.\begin{aligned} B_0 = 0; \quad \varphi(\xi) = \tfrac{D}{B_1^2(\xi)}; \\ D^2\tfrac{1}{B_1^6} - a(\xi)\tfrac{1}{B_1^2} - \tfrac{3}{4} = 0. \end{aligned}\right\} \tag{A 12}$$

After solving this system and satisfying the boundary conditions (A 8) we obtain the final asymptotic solution for the modulation of surface wave by the non-uniform moving current

$$\left.\begin{aligned} \Phi_0(\xi) = B_1(\xi)\cos\left(\sqrt{G_0/G_2}\int_{-1}^{\xi}\frac{D}{B_1^2(\xi)}\mathrm{d}\xi\right), \quad D = \frac{\sqrt{3}}{2}G_0^{-3/2}; \\ B_1(\xi) = \left(\frac{4D^2}{3}\right)^{1/6} \\ \times \frac{1}{\{(1/2 + (1/4 - 2^4/3^5 a(\xi)^3/D^2)^{1/2})^{1/3} + (1/2 - (1/4 - 2^4/3^5 a(\xi)^3/D^2)^{1/2})^{1/3}\}^{1/2}}. \end{aligned}\right\} \tag{A 13}$$

This solution can be simplified in the main region of the positive current where $u(\xi) \sim O(1)$:

$$\Phi_0(\xi) = \left(\frac{\sqrt{3}}{2}\right)^{1/2} \frac{1}{G_0^{3/4}} \frac{\cos\left(\sqrt{G_0/G_2}\int_{-1}^{\xi} u(\xi)^{1/2}\mathrm{d}\xi\right)}{u(\xi)^{1/4}}. \tag{A 14}$$

The last expression corresponds to the well-known WKB asymptotic solution (Naiphe 1981) consistent with the linear form of the Schrödinger equation (4.4).

A first-order solution for the SW modulation on a counterflow $u(\xi) < 0$ can be found in the following algebraic form:

$$\Phi_0(\xi) = \sqrt{1/G_0 - u(\xi)}. \tag{A 15}$$

The next order of approximation $\Phi_1(\eta, \xi)$ results in (A16):

$$\frac{\partial^2 \Phi_1}{\partial \eta^2} + 2\Phi_0^2(\xi)\Phi_1 = 0, \tag{A 16}$$

where function $\varphi(\xi)$ (see expression (A 2)) is set equal to unity.

This is the linear Schrödinger equation, containing the slow varying parameter $2\Phi_0^2(\xi)$ at the potential. The potential function does not change the sign. Consequently, we apply a standard WKB method (Nayfeh 1981) to find its asymptotic solution:

$$\Phi_1 = D_1 \frac{\sin\left(\sqrt{G_0/G_2}\int_{-1}^{\xi}\sqrt{2}\Phi_0\mathrm{d}\tau\right)}{(\sqrt{2}\Phi_0)^{1/2}} + D_2 \frac{\cos\left(\sqrt{G_0/G_2}\int_{-1}^{\xi}\sqrt{2}\Phi_0\mathrm{d}\tau\right)}{(\sqrt{2}\Phi_0)^{1/2}}, \tag{A 17}$$

where D_1 and D_2 are constants determined from the boundary conditions (A 8): $D_2 = 0$, $D_1 = -\sqrt{G_2/G_0}\Phi_{0\xi}(-1)/(\sqrt{2}\Phi_0(-1))^{1/2}$.

A.2. An asymptotic solution of (5.2)

Equation (5.2) of the resonant excitatory SW,

$$\phi_{0\xi\xi} + G_I(u(\xi) - \lambda)\phi_0 + \phi_0^3 = 0, \tag{A 18}$$

is analysed under zero boundary conditions (5.1):

$$\phi_0 \to 0 \quad \text{as} \quad u(\xi) \to 0, \quad \xi \to \pm\infty. \tag{A 19}$$

The approach used to find the asymptotic solution of (A 18) appears as follows. Outside the normalized space region of subsurface current $(-1, 1)$ the only solution that satisfies the zero boundary conditions at infinity (A 19) is the soliton of the nonlinear Schrödinger equation:

$$\phi_{0e} = \frac{(2G_I\lambda)^{1/2}}{\cos\mathrm{h}((G_I\lambda)^{1/2}\xi)}. \tag{A 20}$$

This external solution ϕ_{0e} has to be merged with the internal ϕ_{0i} inside the IW current region. The soliton solution exists only for positive values of the parameter $\lambda > 0$. This means that C, the phase velocity of IW, has to be less than the linear group velocity of the excited surface waves, i.e. $C < c_g$.

The internal asymptotic solution of (A 19) inside the interval $(-1, 1)$ ϕ_{0i} can be constructed in the same way as in § 4. Let us consider first the SW excitation on the countercurrent $u(\xi) < 0$.

The solution can be expressed as an asymptotic series:

$$\phi_{0i}(\xi) = G_0^{1/2}\phi_{00}(\xi) + \phi_{01}(\xi) + \cdots. \tag{A 21}$$

After substituting the expression (A 21) into (A 18), equaling the same order values and applying the standard WKB technique for second-order equation, we obtain

$$\phi_{0i}(\xi) = G_I^{1/2}(\lambda - u(\xi))^{1/2} + D_1 \frac{\sin\left(G_I^{1/2}\int_{-1}^{\xi}\sqrt{2}(\lambda - u(\tau))^{1/2}\mathrm{d}\tau\right)}{(\lambda - u(\xi))^{1/4}} + D_2 \frac{\cos\left(G_I^{1/2}\int_{-1}^{\xi}\sqrt{2}(\lambda - u(\tau))^{1/2}\mathrm{d}\tau\right)}{(\lambda - u(\xi))^{1/4}}, \tag{A 22}$$

where D_1, D_2 are the constants to be determined from the conditions imposed by smooth merging with the external solution (A 20) at the left boundary point $\xi = -1$: $\phi_{0i}(-1) = \phi_{0e}(-1); \phi_{0\xi i}(-1) = \phi_{0\xi e}(-1)$. These values are found as follows:

$$D_1 = \frac{1}{\sqrt{2}\lambda^{1/4}G_I^{1/2}}\left(\phi_{0\xi e}(-1) - D_2\lambda^{-5/4}/4 - u_\xi(-1)G_I^{1/2}\lambda^{-1/2}/2\right),$$
$$D_2 = \lambda^{1/4}\left(\phi_{0e}(-1) - \lambda^{1/2}G_I^{1/2}\right).$$

The following integral relationship follows from (A 22) to fulfill the smooth transition between the internal solution (A 22) and the external solution (A 20) at the right boundary point $\xi = 1$ (we assume that the current function $u(\xi)$ is even):

$$G_I^{1/2}\int_{-1}^{1}\sqrt{2}(\lambda - u(\tau))^{1/2}\mathrm{d}\tau = 2\pi n, \tag{A 23}$$

where $n = 1, 2, 3, \ldots$ are arbitrary positive integers.

This implies the existence of the dynamic threshold of IW for the excitation of various different modes of surface waves. To analyse (A 23) in detail we rewrite it in a dimensional form:

$$G_I^{1/2}\left(\frac{L}{2\sqrt{2}}\right)^{-1}\int_{-L/2}^{L/2}\left(1 - \frac{2U(\xi)}{C} - \left(\frac{2C}{c_p}\right)^2\left(1 - \frac{U(\xi)}{C}\right)\right)^{1/2}\mathrm{d}\xi = 2\pi n. \tag{A 24}$$

The only free parameter in the left side of (A 24) for the fixed IW is the SW phase velocity c_p, which has to be larger than $2C(\lambda > 0)$. Equation (A 24) defines the discrete spectrum of surface waves which can now be excited by the IW. The lower limit of the function under the integral is $(-U(\xi)/C)^{1/2}$ (this is the lowest threshold for SW excitation). We reach this scenario under the phase resonance conditions $c_p = 2c_g \to 2C$. The upper limit $(1 - U(\xi)/C)^{1/2}$ and the highest threshold is reached for a relatively long SW $c_p \gg 2C$. The lowest excited SW mode corresponds to $n = 1$ and higher modes can be generated by increasing the intensity and space scale of IW.

REFERENCES

Alpers, W. 1985 Theory of radar imaging of internal waves. *Nature,* **314**, 245–247.

Andonovati, As., Karjanto, N. & Groesen van, E. 2007 Extreme wave phenomena in down-stream running modulated waves. *Appl. Math. Model.* **31**, 1425–1443.

Bakhanov, V. V., Belyakhov, D. L., Ryabinin, A. G., Titov, V. I. & Zuikova, E. M. 1994 Nonlocal effect of internal waves on the ocean surface. In *Geoscience and Remote Sensing Symposium, IGARSS '94. Surface and Atmospheric Remote Sensing: Technologies, Data Analysis and Interpretation., International,* **2**, 760–762.

Bakhanov, V. V. & Ostrovski, L. A. 2002 Action of strong internal solitary waves on surface wave. *J. Geophys. Res.* **107**(C10), 3139.

Basovich, A. Y., Bachanov, V. V., & Talanov, V. I. 1987 Transformation of wind-driven wave spectra by short internal wave trains. *Izv., Acad. Sci., USSR, Atmos. Oceanic Phys.* **23**(7), 520–528.

Chereskin, T. & Mollo-Christensen, E. 1985 Modulational development of nonlinear gravity wave groups. *J. Fluid Mech.* **154**, 337–365.

Donato, A. N., Peregrine, D. H. & Stocker, J. R. 1999 The focusing of surface. waves by internal waves. *J. Fluid Mech.* **384**, 27–58.

Gargett, A. E. & Hughes, B. A. 1972 On the interaction of surface and internal waves. *J. Fluid Mech.* **52**, 179–191.

Gasparovic, R. F., Apel, J. R. & Kasischke, E. S. 1988 An overview of the SAR internal wave experiment. *J. Geophys. Res.* **93**, 12 304–12, 315.

Hogan, G. G., Chapman, R. D., Watson, G. & Thompson, D. R. 1996 Observations of ship-generated internal waves in SAR images from Loch Linnhe, Scotland, and comparison with theory and in situ internal wave measurements. *IEEE Trans. Geosci. Remote Sens.* **34**, 532–542.

Holliday, D. 1973 Nonlinear gravity-capillary surface waves in **a** slowly varying current. *J. Fluid Mech.* **57**, 797–802.

Hughes, B. A. 1978 The effect of internal waves on surface wind waves. 2, Theoretical analysis. *J. Geophys. Res.* **83**, 455–465.

Hughes, B. A. & Grant, H. L. 1978 The effect of internal waves on surface wind waves. I: Experimental measurements. *J. Geophys. Res.* **83**, 443–454.

Karjanto, N. & Groesen E. 2007 Note on wavefront dislocation in surface water waves. *Phys. Lett.* A **371**, 173–179.

Kropfli, R. A., Ostrovski, L. A., Stampton, T. P., Skirta, E. A., Keane, A. N. & Irisov, V. 1999 Relationships between strong internal waves in the coastal zone and their radar and radiometric signatures. *J. Geophys. Res.* **104(**C2), 3133–3148.

Kuzmak, J. E. 1959 Asymptotic solutions of nonlinear second order differential equations with variable coefficients. *Appl. Math Mech.* **23**, 730–744.

Landau, L. & Lifshitz, E. 1977 *Quantum Mechanics (non-relativistic theory): Course of Theoretical Physics*, Vol. 3. Elsevier.

Lewis, J. E., Lake, B. M., & Ko, D. R. 1974 On the interaction of internal waves and surface gravity waves. *J. Fluid Mech.* **63**, 773.

Longuet-Higgins, M. S. & Stewart, R. W. 1964 Radiation stress in water waves, a physical discussion with application. *Deep-Sea Res.* **11**, 529–562.

Luke, J. C. 1966 A perturbation method for nonlinear dispersive wave problems. *Proc. R. Soc. Lond. Ser.* A*: Math. Phys. Sci.* **292** (1430), 403–412.

Melville, W. 1983 Wave modulation and breakdown. *J. Fluid Mech.* **128**, 489–506.

Nayfeh, A. H. 1981 *Introduction to Perturbation Techniques*. John Wiley & Sons.

Osborne, A. R. & Burch, T. L. 1980 Internal solitons in the Andaman Sea. *Science* **208**, 451–460.

Phillips, O. M. 1974 Nonlinear dispersive waves. *Annu. Rev. Fluid Mech.* **6**, 93–110.

Phillips, O. M. 1977 *Dynamics of the Upper Ocean Layer*. John Wiley & Sons.

Shugan, I. & Voliak, K. 1998 On phase kinks, negative frequencies and other third order peculiarities of modulated surface waves. *J. Fluid Mech.* **368**, 321–338.

Smith, R. 1976 Giant waves. *J. Fluid Mech.* **77**, 417–431.

Stocker, J. R. & Peregrine, D. H. 1999 Three-dimensional surface. waves propagating over long internal waves. *European J. Mech.* B/*Fluids* **18**, 545–559.

Watson, G., Chapmen, R. D. & Apel, J. R. 1992 Measurements of the internal wave wake of a ship in a highly stratified sea Loch. *J. Geophys. Res.* **97** (C6), 9689–9703.

Whitham, G. B. 1974 *Linear and Nonlinear Waves*. John Wiley & Sons.

Yuen, H. C. & Lake, B. M. 1982 Nonlinear dynamics of deep-water gravity waves. In *Advances in Applied Mechanics* **22**, pp. 67–229. Academic Press.